A Hybrid Continuum-Kinetic Approach for High Altitude Rocket Exhaust Plume Simulation

Ursula Rasthofer
IABG mbH
Einsteinstraße 20, 85521 Ottobrunn
GERMANY

rasthofer@iabg.de

Phillip Ohmer
IABG mbH
Einsteinstraße 20, 85521 Ottobrunn
GERMANY

ohmer@iabg.de

Hartmut Siegmann
IABG mbH
Einsteinstraße 20, 85521 Ottobrunn
GERMANY

siegmann@iabg.de

ABSTRACT

Flow simulation of rocket exhaust plumes, in particular at high flight altitude, presents formidable challenges to high-fidelity simulations. Reliable predictions of rocket exhaust plume flow fields are of great importance for the successful analysis of missile infrared signatures. The majority of computational studies focus on low-altitude flights, where continuum approaches based on the Navier-Stokes equations are assumed to be valid in the entire flow field. At high altitudes, thermodynamic non-equilibrium effects are encountered in the flow past the missile as well as further downstream of the nozzle exit. A kinetic approach, such as the Direct Simulation Monte Carlo (DSMC) method, has to be applied in order to obtain reliable information on these rarefied gas flows. Theoretically, the DSMC approach is also valid in the low-Knudsen-number regime of continuum flows. However, methodical requirements render the DSMC method computationally prohibitive in the continuum limit. Rocket exhaust plumes at high altitudes exhibit Knudsen numbers typically ranging from approximately 10^{-6} at the nozzle exit to about 10 in the incident flow. Owing to the pronounced multiscale character of rocket exhaust plume flows, hybrid approaches, combining continuum methods for the flow in the vicinity of the nozzle exit with kinetic methods for the surrounding rarefied gas flow, constitute a reasonable procedure for achieving credible and computationally efficient simulations. In this study, a one-way-coupled hybrid continuum-kinetic approach is suggested for high altitude rocket exhaust plume simulation. Apart from the derivation of appropriate boundary conditions for the transfer of flow information across the hybrid interface separating the Navier-Stokes and the DSMC domain, consistency in the thermo-chemical models is additionally required for a high-quality hybrid solution. Therefore, consistency in the chemical reaction rate is particularly addressed, as it is of paramount importance in the case of post-combustion within the exhaust plume split by the hybrid interface. The proposed method is then applied to a reacting rocket exhaust plume simulation at an altitude of 114 km.

1.0 INTRODUCTION

When dealing with rarefied gas dynamics as encountered for flights at high altitudes, the DSMC method has evolved to a reliable simulation approach; see., e.g., [1–3]. Although theoretically valid for continuum gas flows, the computational efficiency of the DMSC method notably worsens with decreasing Knudsen numbers. As a results, both low-Knudsen-number extensions for the DSMC approach as well as hybrid schemes which apply the DSMC method only to rarefied regions and utilize Navier-Stokes-based schemes in continuum regions of the flow field have evolved to deal with flows involving a wide range of Knudsen number regimes. Low-Knudsen-number extensions of the DSMC method usually rely on approximations for the collision integral of the Boltzmann equation such as the Bhatnagar-Gross-Krook (BGK) model [4] or the Fokker-Planck (FP) model [5]. In, e.g., [6–8], these approximations are used to derive a modified collision procedure for DSMC-based schemes. Instead of evaluating binary collisions between randomly selected particles from a collision cell, all particles are relaxed based on a temperature and viscosity dependent probability to a target distribution function, e.g., the Maxwellian velocity distribution. BGK-DSMC method and FP-DSMC methods distinguish cells where particle collisions are executed as usual and cells where approximative, and thus, less expensive procedures are applied. The discretisation between classical DSMC cells and BGK or FP cells is carried out, for instance, based on the local number density or Knudsen number; see, e.g., [9]. Study [9] proposes a combination of the DSMC method and the Equilibrium Particle Simulation Method (EPSM) developed in [10]. In [10], the EPSM is presented as the infinite collision rate or continuum limit of DSMC method. Similar to BGK and FP, the EPSM does not calculate collisions between particles in a cell but incorporates the effect of the collisions redistributing the total momentum and energy of all the particles in a cell amongst all the particles in the selected cell. Therefore, new particle velocities are selected at random from a local Maxwellian equilibrium distribution, while the total momentum and energy are preserved in the selected cell. In contrast, the Low Diffusion (LD) method, originally presented in [11] and later applied together with the DSMC method in a combined approach for rocket exhaust plume simulation in [12], represents a deterministic particle-based continuum method. Hybrid schemes coupling the DSMC method and a grid-based solver for the Navier-Stokes equations are presented, e.g., in [13–15]. The state-based coupling of [14] temporarily averages particle information to obtain a macroscopic state in a cell layer on the DSMC side of the interface and at the same time generates a distribution of particles from a macroscopic state in a cell layer on the Navier-Stokes side of the interface. Flux-based coupling schemes, as, e.g., suggested in [15–17] involve calculating the fluxes of mass, momentum and energy at the interface accordingly. The continuum flux is used to create a distribution of particles at the interface which then propagate into the DSMC domain. Both DSMC method with low-Knudsen-number extensions as well as the aforementioned hybrid schemes rely on the identification of the interface separating the DSMC domain from the continuum domain. This interface is usually defined via an appropriate Continuum-Breakdown-Parameter, as discussed, e.g., in [18, 19]. When dealing with hybrid schemes coupling the DSMC method and a grid-based solver for the Navier-Stokes equations, consistency of the transport coefficients and thermo-chemical model is required for a smooth transition from one domain into the other, as discussed, e.g., in [15]. Furthermore, two-way-coupled approaches, taking into account gas flow from the continuum domain to the DSMC domain and vice versa, additionally suffer from potentially large statistical scatter in conserved macroscopic quantities as calculated from the particles used in the DSMC methods. Techniques to compensate for scatter are investigated, e.g., in [20].

In this study, we present a one-way-coupled hybrid continuum-kinetic approach, using a grid-based approach for solving the Navier-Stokes equation together with the DSMC method in regions of rarefied flow, for high altitude rocket exhaust plume simulation. At high altitudes, the flow in the rocket motor chamber, its nozzle and in the direct vicinity of the rocket nozzle exit are typically still in the continuum flow regime characterized by extremely small Knudsen numbers in the range of about 10^{-6}. As the flow propagates from the nozzle exit to the far field and, hence, from the continuum domain to the DSMC domain a one-way-coupled scheme appears to be sufficient; as also considered in [13, 21]. This procedure also allows for taking into account the chemical reactions of the post-combustion processes occurring in the

exhaust plume in both the continuum and the DSMC domain, which is frequently not supported by low-Knudsen number extension of the DSMC method.

The present paper is organized as follows: Chapter 2.0 develops the hybrid continuum-kinetic method for rocket exhaust plume simulation. The interface extraction is discussed, and further aspects related to the consistency between DSMC- and Navier-Stokes approach are addressed. Computational results of the application of the developed hybrid continuum-kinetic method to rocket exhaust plume simulation are shown in chapter 3.0. The present study is concluded in chapter 4.0.

2.0 HYBRID CONTINUUM-KINETIC METHOD

2.1. Brief Overview of the Numerical Procedures

Before developing the hybrid continuum-kinetic method, a brief overview of the DSMC method and used form of the Navier-Stokes equations is provided. The DSMC method, which recovers the physics of the Boltzmann equation, tracks the motions and collisions of a large number of simulation particles, each representing a large number of atoms or molecules. Apart from its position and velocity vector, each particle exhibits the physical properties of its assigned gas species such as mass and size. Additionally, internal, i.e., rotational and vibrational, energy values are assigned to simulation particles that correspond to molecules. In each time step, particle advection and collisions are treated separately. Therefore, DSMC simulations are inherently transient with a time-step size smaller than the local mean collision time. Furthermore, the computational domain is covered by a grid of cells. These grid cells are used to group collections of particles from which collision partners are chosen at random. Furthermore, they serve for sampling of time-averaged macroscopic properties, i.e., bulk velocity, translational, rotational and vibrational temperature, density, pressure as well as number densities of the considered gas species. During each time step, particle motion is executed fist, while boundary conditions such as reflection from solid surfaces are taken into account. Second, particles are assigned to grid cells according to their current position. Eventually, collision operations among randomly selected pairs of particles within each cell occur. This procedure requires that the cell dimension be less than the local mean free path. Elastic binary collisions result in the velocity changes of the involved particles. The binary collision rate is a function of the collision cross section which is most commonly described by the Variable Hard Sphere (VHS) model [22] and the Variable Soft Sphere (VSS) model [23]. Moreover, exchange of energy between translational and internal energy modes as well as chemical reactions may be applied to some fraction of colliding particles. For chemical reactions, the Total Collision Energy (TCE) model of [24], which is based on modified Arrhenius rate coefficient is widely used in DSMC simulation.

Continuum flow is governed by the compressible flow Navier-Stokes equations which comprise conservation equations for mass, momentum and energy. Neglecting gravitational and body forces, the momentum equation read as:

$$\frac{\partial \rho \vec{u}}{\partial t} + \nabla \cdot (\rho \vec{u}\vec{u}) = -\nabla p + \nabla \cdot \bar{\bar{\tau}}, \tag{1}$$

where ρ, $\vec{u}$, and p represent the fluid density, velocity and pressure, while $\bar{\bar{\tau}}$ represents the viscous shear stress tensor. For the N gas species that comprise the rocket exhaust gas mixture, $N-1$ transport equations are solved in addition to the (mixture) continuity equation. The governing equation for mass transport and conservation of the i-th gas species mass fraction w_i is given by:

$$\frac{\partial}{\partial t}(\rho w_i) + \nabla \cdot (\rho \vec{u} w_i) = -\nabla \cdot \vec{J_i} + R_i, \tag{2}$$

where $\vec{J_i}$ is the diffusion flux vector for the species i and R_i the source term due to chemical reactions in the flow field. The energy conservation equation for the reacting gas mixture involving species enthalpies h_i, their diffusive fluxes and the chemical reaction heat sources S_r is given by:

$$\frac{\partial}{\partial t}\left(\rho\left(e+\frac{|\vec{u}|^2}{2}\right)\right)+\nabla\cdot\left(\rho\vec{v}\left(\sum w_i h_i+\frac{|\vec{u}|^2}{2}\right)\right)=\nabla\cdot\left(k\nabla T-\sum h_i\vec{J_i}+\bar{\bar{\tau}}\cdot\vec{u}\right)+S_r \qquad (3)$$

where k denotes the thermal conductivity while e describes the specific internal energy of the fluid. Chemical reactions are modeled via finite-rate kinetics.

2.2. Coupling Strategy

Rocket exhaust plume flow is typically supersonic with Mach numbers notably larger than unity and directed from the dense continuum region, in the vicinity of the nozzle exit, toward the rarefied mid and far field plume. Therefore, our hybrid continuum-kinetic approach consists of a conceptually simpler one-way coupling strategy from the grid-based Navier-Stokes solver to the particle-based DSMC solver, relying on the negligible upstream influence of points located downstream. A schematic sketch of the unidirectional coupling approach is shown in Figure 2-1. Owing to the transport of information from the continuum to the kinetic flow domain, the Navier-Stokes solution is computed first. The Navier-Stokes equations are solved in a domain covering not only the dense flow behind the nozzle exit but extending into the rarefied incoming flow and the mid-field of the plume as well. This enlarged domain is necessary, as the location of the hybrid interface, separating the computational domains of the Navier-Stokes and the DSMC solver, is unknown a-priori. The hybrid interface is then identified based on the Navier-Stokes solution only.

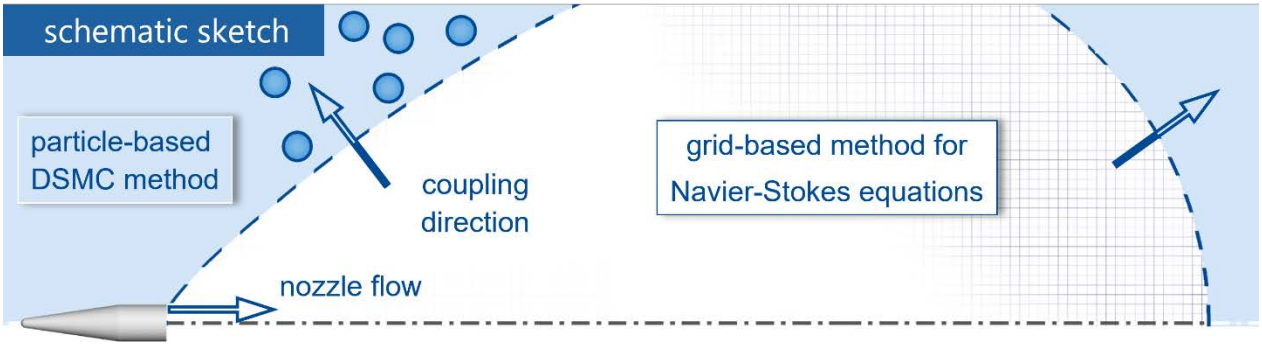

Figure 2-1: Schematic sketch of unidirectional continuum-kinetic coupling.

An appropriate continuum-breakdown parameter defines the interface location within the initially enhanced Navier-Stokes domain. The interface separates the continuum domain from the kinetic domain. The breakdown parameter is usually based on the local mean free path or number density and given in terms of a Knudsen number. A characteristic iso-surface of the breakdown parameter field computed from the Navier-Stokes solution implicitly captures the hybrid interface, which may exhibit an arbitrary shape. Typically used definitions of the continuum breakdown parameter are:

- the local number density.
- the global Knudsen number

$$\mathrm{Kn}=\frac{\lambda}{L_{\mathrm{ref}}}, \qquad (4)$$

  which is based on the local mean free path λ and a characteristic length L_{ref} of the geometry.
- the local gradient-based Knudsen number, as suggested, e.g., in [18, 19],

$$\mathrm{Kn}_{\mathrm{GL}}=\max\left(\mathrm{Kn}_{\mathrm{GL}-\rho},\mathrm{Kn}_{\mathrm{GL}-T},\mathrm{Kn}_{\mathrm{GL}-u},\mathrm{Kn}\right) \qquad (5)$$

  using

$$\mathrm{Kn}_{\mathrm{GL}-Q} = \frac{\lambda}{Q}|\nabla Q|, \tag{6}$$

where Q represents density ρ, temperature T or velocity magnitude u, respectively.

The actual choice of the criterium depends on the considered flow problem. Furthermore, an appropriate iso-value has to be defined; see, e.g., [18, 19] for further discussion.

The present hybrid approach constitutes a combination of a state- and flux-based approach. Therefore, the implicitly defined interface which is an iso-contour of one of the aforementioned fields has to be discretized. As a result of this procedure, the interface is described by a set of connected straight lines in the two-dimensional case and by triangles for three dimensions. At each interface location, the macroscopic flow quantities are extracted from the Navier-Stokes solution. The extracted macroscopic flow quantities are assumed constant on each interface element. Based on the macroscopic flow quantities on the interface, the particle flux across the interface is computed. Following [1], the particle flux $\dot{N}$ across each element of the interface is given by

$$\dot{N} = n_\rho \beta^{-1} \left(\frac{\mathrm{e}^{-(\beta u_\mathrm{n})^2} + \sqrt{\pi}\beta u_\mathrm{n}(1 + \mathrm{erf}(\beta u_\mathrm{n}))}{2\sqrt{\pi}} \right) \tag{7}$$

using

$$\beta^{-1} = \sqrt{\frac{2k_\mathrm{B}T}{m}} \tag{8}$$

where n_ρ denotes the number density, u_n the velocity component normal to the interface, k_B the Boltzmann constant and T the temperature. As similar procedure is used, e.g., in [25] for particle emission at domain boundaries.

After multiplication of the particle flux $\dot{N}$ by the area of the interface element, the time-step size of the simulation and the reciprocal value of particle weight, i.e., the number of gas particles represented by a simulation particle, the number of simulation particles that enter the DSMC domain at the interface element during the present time step is obtained. The seed of the simulation particles at the interface element is based on a Maxwellian velocity distribution.

2.3. Consistent Flow Formulation

In order to guarantee a smooth transition from the continuum domain to the kinetic domain, consistency of the thermo-chemical models at the interface is of paramount importance, as addressed, e.g., in [15]. In the following, consistency of the transport coefficients and the reaction rate model are addressed.

Using the VSS collision model and assuming collision of gas particles of the same species i, the binary dynamic viscosity reads as

$$\mu_i = \frac{15\sqrt{\pi m_i k_\mathrm{B} T_{i,\mathrm{ref}}}}{2(5-2\omega_i)(7-2\omega_i)\pi d_{i,\mathrm{ref}}^2} \frac{(\alpha_i+1)(\alpha_i+2)}{6\alpha_i} \left(\frac{T}{T_{i,\mathrm{ref}}} \right)^{\omega_i}, \tag{9}$$

where $T_{i,\mathrm{ref}}$ and $d_{i,\mathrm{ref}}$ denote the reference temperature and diameter, respectively, and ω_i, α_i are further parameters of the VSS model for species i; see, e.g., [1, 3] for further details. The Boltzmann constant is given by k_B. Analogously, the binary thermal conductivity is obtained as

$$k_i = \frac{15}{4}\left(\frac{k_\mathrm{B}}{m_i}\right)\mu_i, \tag{10}$$

where m_i refers to the molecular mass of species i. Furthermore, mono-atomic gas species are assumed in equation (9) for brevity in the present elaboration. For full presentation, the reader is referred, e.g., to [1, 3]. The resulting binary dynamic viscosities for all considered gas species are set in the continuum approach and combined by appropriate mixing rules. Here, the mixture properties for the dynamic viscosity and the thermal conductivity are approximated via mass weighted averaging based on the binary properties of the gas species and their mass fractions via

$$k_\mathrm{mix} = \sum_i w_i\, k_i, \tag{11}$$

$$\mu_\mathrm{mix} = \sum_i w_i\, \mu_i. \tag{12}$$

Diffusion coefficients are treated analogously.

Likewise, we address chemical reactions in a consistent manner. In the continuum solver, we use the finite rate chemistry model which basically evaluates the gas species source term R_i of equation (2), due to the N_r chemical reactions as the sum over the molar net reaction source rates for each reaction r and the species molar mass M_i:

$$R_i = M_i \sum_{r=1}^{N_r}\left[\left(\nu''_{i,r} - \nu'_{i,r}\right)\left(k_{\mathrm{f},r}\prod_{j=1}^{N} C_{j,r}^{n'_{j,r}} - k_{\mathrm{b},r}\prod_{j=1}^{N} C_{j,r}^{n''_{j,r}}\right)\right], \tag{13}$$

where $\nu_{i,r}$ is the stoichiometric coefficient for a reactant i in reaction r. The forward and backward rates $k_{\mathrm{f},r}$ and $k_{\mathrm{b},r}$, respectively, are determined by applying Arrhenius rate laws for the forward reaction and estimating the backward reaction rate via the equilibrium constant as usual. $C_{j,r}$ represents the molar concentration of species j in the reaction with $n_{j,r}$ being the corresponding rate exponent. Properties of reactants are marked by $'$, while reaction products are indicated by $''$. The reaction energy source term S_r in equation (3) may be evaluated using the volumetric species source term and the species enthalpy of formation h_i^0 as:

$$S_r = -\sum_i \frac{h_i^0}{M_i} R_i. \tag{14}$$

To achieve consistency between continuum and kinetic approach, we apply the TCE model in the DSMC method. The TCE model is closely related to the finite rate model of the continuum solver as both are based on the Arrhenius rate laws to determine the reaction kinetics. Especially for the case $T_\mathrm{tra} = T_\mathrm{rot} = T_\mathrm{vib} = T$, where translational, rotational and vibrational temperatures are equal, the TCE model reproduces the forward reaction rates $k_{f,r}$ of the continuum finite rate model. The TCE approach models the probability of a chemical reaction P_react as a function of the available total collision energy E_coll of the particles participating in the collision and the activation energy E_A of the reaction:

$$P_\mathrm{react} = \begin{cases} 0 & \text{for } E_\mathrm{coll} \le E_\mathrm{A}, \\ C_1 (E_\mathrm{coll} - E_\mathrm{A})^{C_2}\left(1 - \dfrac{E_\mathrm{A}}{E_\mathrm{coll}}\right)^{C_3} & \text{for } E_\mathrm{coll} > E_\mathrm{A}. \end{cases} \tag{15}$$

where the three coefficients C_1, C_2 and C_3 are determined using the Arrhenius rate coefficients, the average number of degrees of freedom of the participating particles as well as the parameters of the VSS collision model. In TCE model both forward and backward reaction rate have to be provided in Arrhenius form, so fitting of the finite rate chemistry backward rate might be required.

3.0 COMPUTATIONAL RESULTS

The presented hybrid continuum-kinetic method for multiscale Knudsen number problems spanning over several orders of magnitude is realized using the DSMC software SPARTA, as presented in [25], together with ANSYS© Fluent© for continuum flow governed by the Navier-Stokes equation.

3.1. 2D Jet Flow

To verify the hybrid continuum-kinetic approach developed in the previous chapter, the two-dimensional jet flow described in [2] is considered. The Knudsen number for this flow is of the order of $O(10^{-4})$ such that both continuum and kinetic approaches can be applied to the flow problem. Following [2], the velocity of the jet at the nozzle exit amount to 372 m/s, the temperature to 300 K and the number density to $9.98 \cdot 10^{21}$ m^{-3}. First, the flow is computed in the entire computational domain using the DSMC method, as shown for the horizontal velocity field in upper part of Figure 3-1. Using this result, an interface is defined based on an iso-contour of the number density field, where $n_\rho = 4.8 \cdot 10^{21} m^{-3}$. Macroscopic data are extracted at the interface and used as interface conditions for a second simulation with interface; see the lower part of Figure 3-1. As expected, differences in the solution field are not stateable.

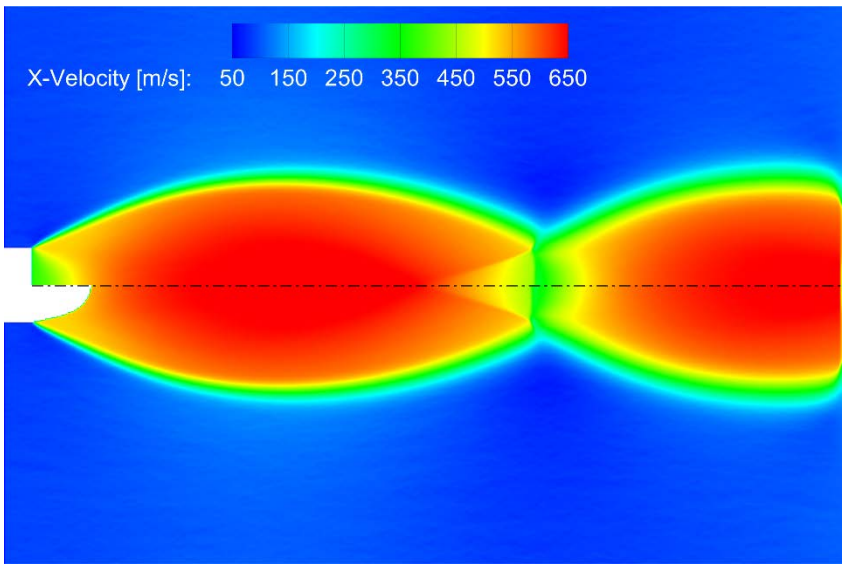

Figure 3-1: Horizontal velocity field of 2D jet flow (top: full solution, bottom: solution based on extracted interface data).

Additionally, Figure 3-2 shows the horizontal and vertical velocity, temperature as well as number density extracted along the symmetry line of the two-dimensional jet flow with and without interface. The DSMC simulation starting from the interface perfectly reproduces the results of the original simulation on the entire domain, demonstrating the accuracy of the proposed method.

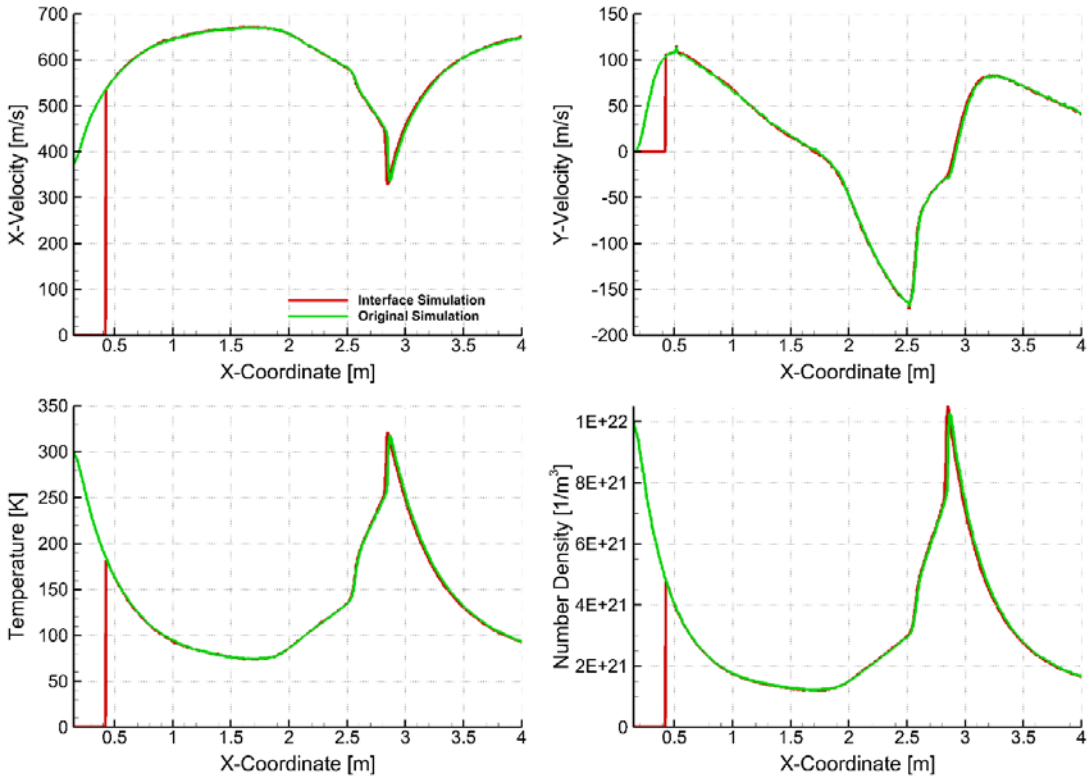

Figure 3-2: Horizontal and vertical velocity, temperature as well as number density extracted from 2D jet flow with and without interface.

3.2. Rocket Exhaust Plume Simulation

In order to test our coupled approach on a full-scale simulation problem, we use a simulation setup similar to [26], which follows one of the only available experiments for a high altitude rocket motor plume shown in [27] for the sounding rocket Strypi XI system. For simulation, we follow [26] by selecting a trajectory point at an altitude of 114 km with the Strypi XI upper stage Star-27 motor being active. Based on [26] and the Star-27 motor geometry, we use the simplified upper stage geometry as shown in Figure 3-3 for our numerical simulations.

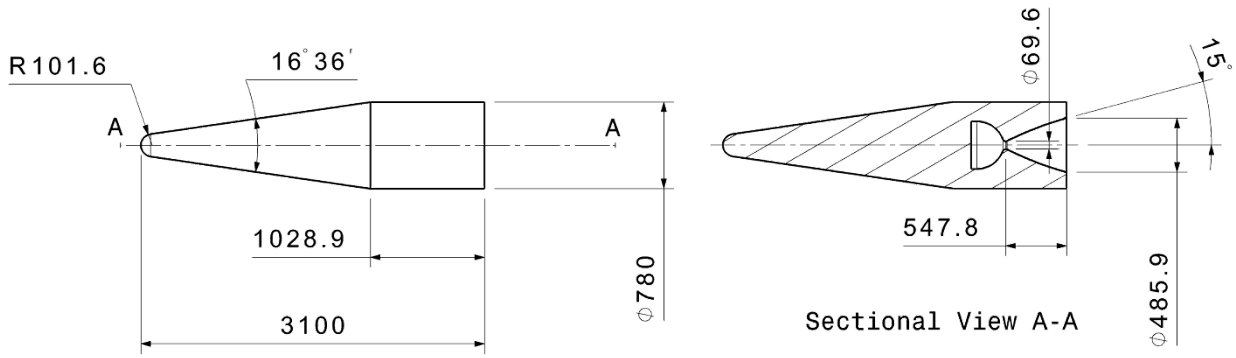

Figure 3-3: Upper stage geometry of the Strypi XI used for hybrid simulations

We apply the same atmospheric ambient gas mixture and flow conditions as specified in [26]. The ambient gas is given by a mixture of 0.78 mol factions N_2 and 0.22 mol fractions O_2 at 288 K temperature and a free stream Mach number of 13.5. Deviating from [26], we model the rocket motor exhaust gas using a larger number of 13 gas components and take 25 possible post-combustion reactions into account. At the chamber

inlet boundary, we apply the combustion gas composition as specified in Table 3-1 at a temperature of about 3442 K and pressure of 3.88 MPa.

Table 3-1: Combustion gas composition at chamber inlet

Gas components:								
Cl	CO	CO_2	H	H_2	H_2O	HCl	OH	N_2
Mass fractions:								
$1.69 \cdot 10^{-4}$	$3.01 \cdot 10^{-1}$	$8.68 \cdot 10^{-2}$	$9.32 \cdot 10^{-6}$	$2.66 \cdot 10^{-2}$	$1.43 \cdot 10^{-1}$	$3.20 \cdot 10^{-1}$	$5.16 \cdot 10^{-6}$	$1.23 \cdot 10^{-1}$

Using the gas mixture specified in Table 3-1 for the rocket chamber and nozzle exit flow and the ambient gas mixture for the ambient background flow, we solve the flow field in two basic steps. As a first step we compute the flow in the rocket chamber, the nozzle flow and the immediate near field of the plume expansion region using the continuum solver Ansys© Fluent©. As outlined in chapter 2.0, the continuum solver also computes the solution for the surrounding rarefied flow region of the ambient background flow. In order to reduce computational cost, we exploit the inherent rotational symmetry of the flow problem at hand. Figure 3-4 shows temperature field in the vicinity of the Strypi XI upper stage of the continuum flow solution only. Apart from a notable outer shock layer due to the interaction of the plume with the ambient flow, a pronounced bow shock at the nose of upper rocket stage geometry is clearly observable.

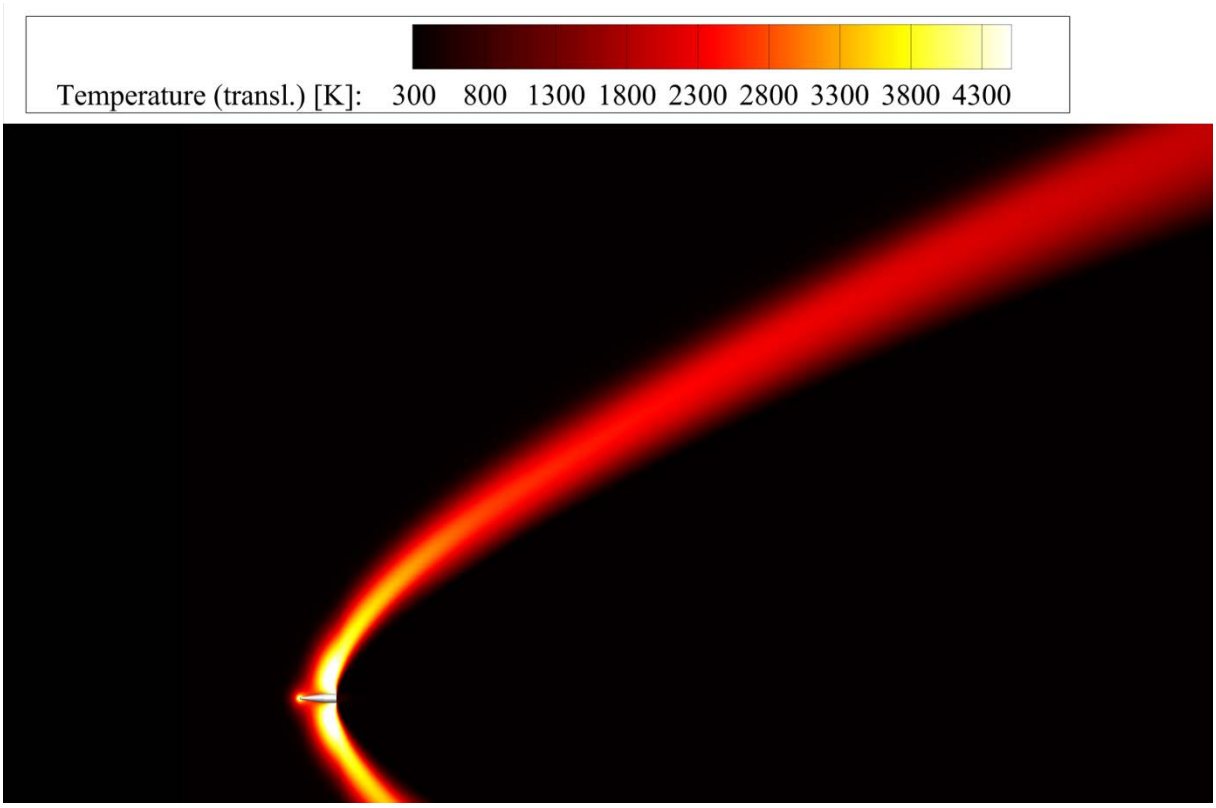

Figure 3-4: Contour plot of the continuum temperature field in the vicinity of the Strypi XI rocket

Next, we solve for the kinetic flow region using the DSMC solver SPARTA©. For this step, we identify the location of the interface separating the continuum domain from the kinetic domain using the breakdown parameters previously discussed. The coupling interface is positioned slightly on the continuum region side.

To capture the entire plume which extends several kilometers downstream of the nozzle exit, a hierarchy of 5 consecutive simulation domains are solved one after the other by DSMC.

Analogously to Figure 3-4, Figure 3-5 shows a close-up of the translational temperature field in the vicinity of the Strypi XI upper stage obtained with the hybrid approach. Merely a weak interaction of the outer shock layer with the bow shock at the nose of upper rocket stage geometry is observable. Instead, the outer shock layer is notably thicker than in the pure continuum simulation result. The size of the Strypi XI upper stage is of the order of the mean free path and has, therefore, hardly any influence on the macroscopic plume structure. This feature cannot be captured in the continuum approach. Additionally, Figure 3-6 displays the full picture of the exhaust plume of the Strypi Xi upper stage. For illustration purposes, the rotational temperature field in the center plane of the plume is depicted. The flow field is computed up to 5 km downstream of the nozzle exit of the Strypi XI upper stage. At this distance, the plume has not yet fully dissipated in the ambient air flow. The notable characteristic is the outer shock layer due to the displacement of supersonic ambient air flow by the expanding exhaust flow. The ability to determine the position and strength of this interaction shock layer is one of the central key features of our approach as it in turn determines the overall resulting shape and dimensions of the rocket exhaust plume flow at high altitudes. At about 2.5 km downstream of the nozzle exit, the core of the plume is compressed resulting in a slight increase of the temperature.

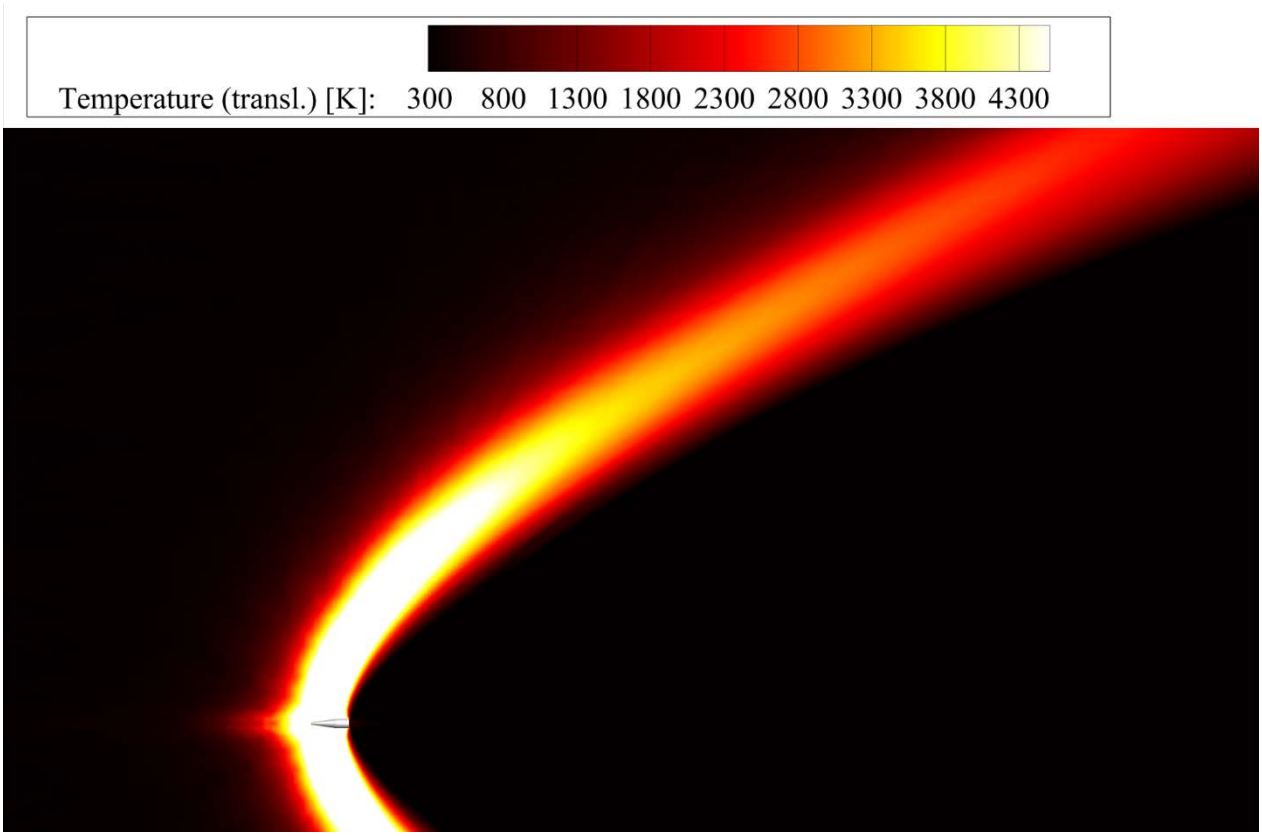

Figure 3-5: Contour plot of the hybrid translational temperature field in the vicinity of the Strypi XI rocket

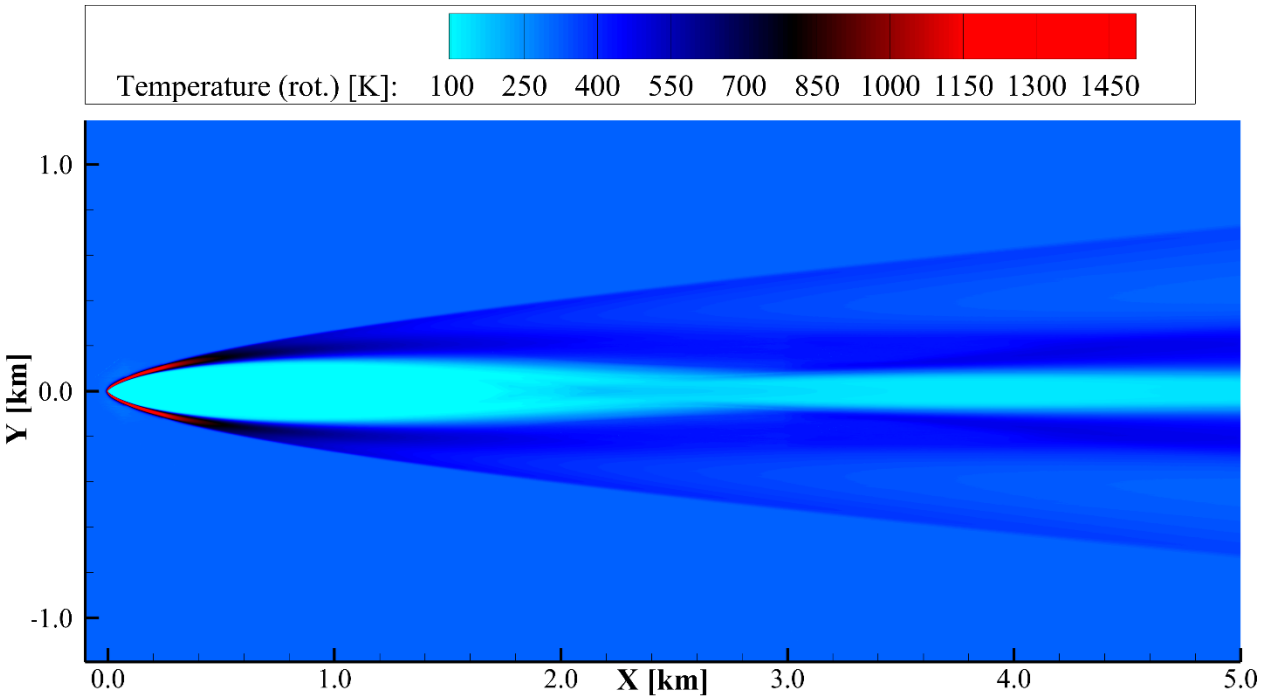

Figure 3-6: Contour plot of the hybrid rotational temperature field in the Strypi XI exhaust plume

Figure 3-7 displays the mass fraction distribution of CO_2 in the upper part and H in the lower part. The CO_2 distribution is a good indicator for identifying the rocket exhaust gases as compared to the ambient air flow, as we modeled the ambient flow mixture without any CO_2 component. On the other hand, atomic H is not present in the flow a priori at all but is created and destroyed only due to the involved chemical reactions. It thus serves as a first indicator to highlight flow regions where chemical reaction processes are occurring. According to Figure 3-7, these reactions seem to occur mainly in the mixing region between the inner expanding jet core and the outer shock layer as well as in the zone of recompression at the tail of the plume core flow.

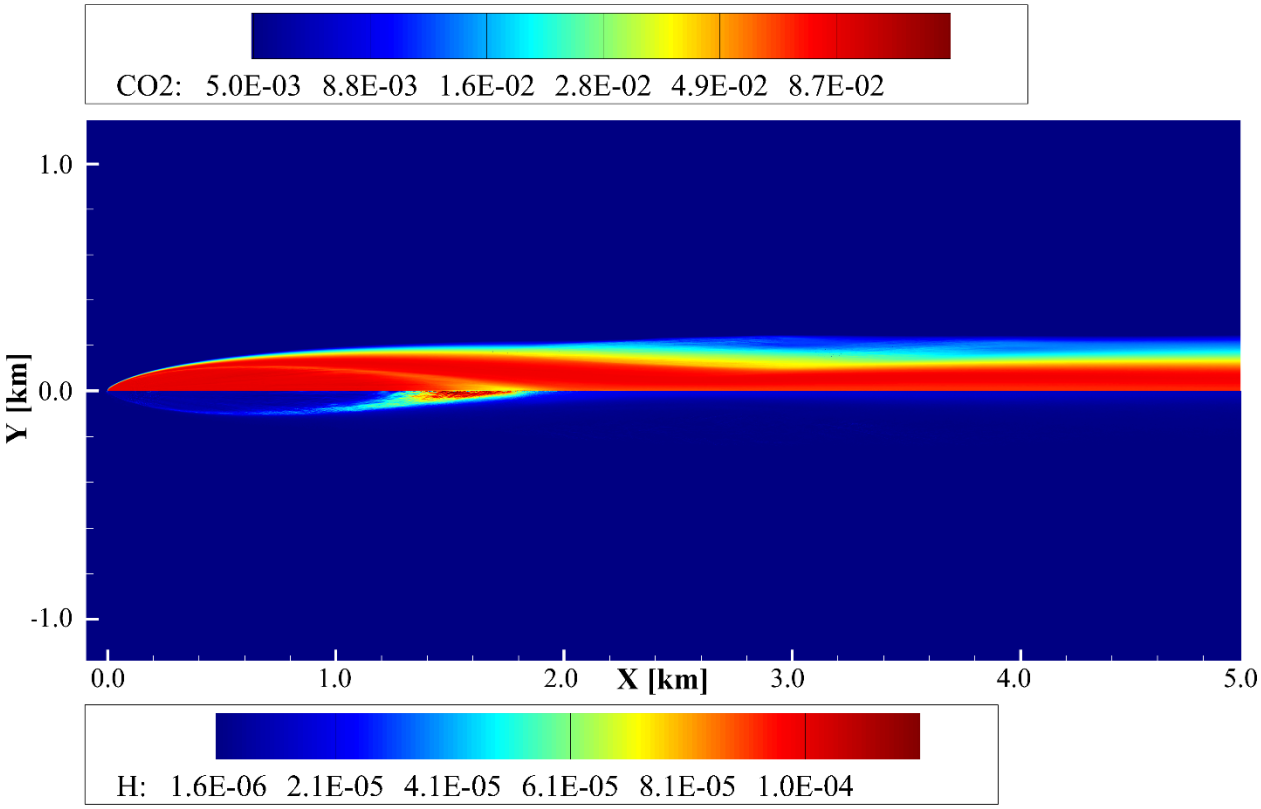

Figure 3-7: Contour plot of CO_2 (top) and H (bottom) hybrid mass fraction fields in the Strypi XI exhaust plume

4.0 CONCLUSIONS

In this study, a one-way-coupled hybrid continuum-kinetic approach using a grid-based method for the Navier-Stokes equations together with the DSMC method for multiscale flow problems, where the Knudsen number range covers several orders of magnitude, is presented. This hybrid continuum-kinetic approach is particularly suited for the simulation of rocket exhaust plume flow at high altitudes. While continuum flow with Knudsen numbers of the order of 10^{-6} is encounter in the vicinity of the nozzle exit, the flow past the rocket as well as further downstream of the nozzle exit is highly rarefied. The one-way-coupled scheme relies on the unidirectional exhaust plume flow from the continuum domain to the DSMC domain. The presented method includes chemical reactions in both the continuum domain and the DSMC domain. Properly set Arrhenius rate coefficients ensure consistency of the applied TCE model of the DSMC method in the limit of continuum flow with the finite rate chemistry model used in the Navier-Stokes equations. Furthermore, transport coefficients occurring in the Navier-Stokes equations, such as viscosity and thermal conductivity, are calculated from species-based values obtained from the binary collisions in the kinetic theory framework using appropriate mixing rules.

Selected numerical results have demonstrated the performance of the presented one-way-coupled hybrid continuum-kinetic approach. In particular, the proposed method has been applied to an exhaust plume simulation for the upper stage of the Strypi XI rocket system at an altitude of 114 km. Chemical reactions and internal energies have been taken into account.

ACKNOWLEGDEMENT

This research was partially supported by the Wehrtechnische Dienststelle für Informationstechnologie und Elektronik (WTD 81) via the contract E/E810/JC032/HF074. This support is gratefully acknowledged. Furthermore, the authors thank Dr. Sebastian Teich of WTD 81 as well as Dr. Daniel Kliche and Denis Zetzmann of IABG for their continuing support and inspiring discussions.

REFERENCES

[1] G. A. Bird, *Molecular gas dynamics and the direct simulation of gas flows*. Oxford: Oxford University Press, 1994.

[2] G. A. Bird, *The DSMC method*, 1st ed.: CreateSpace Independent Publishing Platform, 2013.

[3] I. D. Boyd and T. E. Schwartzentruber, *Nonequilibrium gas dynamics and molecular simulation*. Cambridge: Cambridge University Press, 2017.

[4] P. L. Bhatnagar, E. P. Gross, and M. Krook, "A model for collision processes in gases. I. Small amplitude processes in charged and neutral one-component systems," *Physical Review*, 94(3), pp. 511–525, 1954.

[5] R. F. Pawula, "Approximation of the linear Boltzmann equation by the Fokker-Planck equation," *Physical Review*, 162(1), pp. 186–188, 1967.

[6] M. A. Gallis and J. R. Torczynski, "Investigation of the ellipsoidal-statistical Bhatnagar–Gross–Krook kinetic model applied to gas-phase transport of heat and tangential momentum between parallel walls," *Physics of Fluids*, 23(1), p. 30601, 2011.

[7] E. Jun, M. H. Gorji, M. Grabe, and K. Hannemann, "Assessment of the cubic Fokker–Planck–DSMC hybrid method for hypersonic rarefied flows past a cylinder," *Computers and Fluids*, 168(1), pp. 1–13, 2018.

[8] M. Pfeiffer, "Particle-based fluid dynamics: Comparison of different Bhatnagar-Gross-Krook models and the direct simulation Monte Carlo method for hypersonic flows," *Physics of Fluids*, 30(1), p. 106106, 2018.

[9] M. N. Macrossan, "A particle-only hybrid method for near-continuum flows," in *Proceedings of 22nd International Symposium on Rarefied 2001*, pp. 388–395.

[10] D. I. Pullin, "Direct simulation methods for compressible ideal gas flow," *Journal of Computational Physics*, 34(1), 231-144, 1980.

[11] J. M. Burt and I. D. Boyd, "A Low Diffusion Particle Method for Simulating Near-Equilibrium Flows," *39th AIAA Thermophysics Conference*, AIAA 2007-4259, pp. 1–16, 2007.

[12] J. M. Burt and I. D. Boyd, "A hybrid particle approach for continuum and rarefied flow simulation," *Journal of Computational Physics*, 228(2), pp. 460–475, 2009.

[13] N. E. Gimelshein, R. Lyons, J. Reuster, and S. F. Gimelshein, "Numerical Prediction of UV Radiation from Two-Phase Plumes at High Altitudes," *45th AIAA Aerospace Sciences Meeting and Exhibit*, AIAA 2007-1014, pp. 1–14, 2007.

[14] T. E. Schwartzentruber, L. C. Scalabrin, and I. D. Boyd, "A modular particle–continuum numerical method for hypersonic non-equilibrium gas flows," *Journal of Computational Physics*, 225(1), pp. 1159–1174, 2007.

[15] K. A. Stephani, D. B. Goldstein, and P. L. Varghese, "Generation of a hybrid DSMC/CFD solution for gas mixtures with internal degrees of freedom," *50th AIAA Aerospace Sciences Meeting including the New Horizons Forum and Aerospace Exposition*, AIAA 2012-0648, pp. 1–21, 2012.

[16] H. S. Wijesinghe and N. G. Hadjiconstantinou, "Discussion of Hybrid Atomistic-Continuum Methods for Multiscale Hydrodynamics," *International Journal for Multiscale Computational Engineering*, 2(1), pp. 189–202, 2004.

[17] D. B. Hash and H. A. Hassan, "Assessment of schemes for coupling Monte Carlo and Navier-Stokes solution methods," *Journal of Thermophysics and Heat Transfer*, 10(2), pp. 242–249, 1996.

[18] W. Wang and I. D. Boyd, "Predicting continuum breakdown in hypersonic viscous flows," *Physics of Fluids*, 15(1), pp. 91–100, 2003.

[19] I. D. Boyd, G. Chen, and G. V. Candler, "Predicting failure of the continuum fluid equations in transitional hypersonic flows," *Physics of Fluids*, 7(1), pp. 210–219, 1995.

[20] Q. Sun and I. D. Boyd, "Evaluation of macroscopic properties in the Direct Simulation Monte Carlo method," *Journal of Thermophysics and Heat Transfer*, 19(3), pp. 329–335, 2005.

[21] D. B. van Gilder, C. C. Chartrand, J. Papp, R. Wilmoth, and N. Sinha, "Computational modeling of nearfield to farfield plume expansion," *43rd AIAA/ASME/SAE/ASEE Joint Propulsion Conference & Exhibit*, AIAA 2007–5704, 1, 2007.

[22] G. A. Bird, “Monte Carlo simulation in an engineering context,” *Progress in Astronautics and Aeronautics*, 74(1), pp. 239–255, 1981.
[23] K. Koura and H. Matsumoto, “Variable soft sphere molecular model for air species,” *Physics of Fluids A*, no. 4, pp. 1083–1085, 1992.
[24] G. A. Bird, “Simulation of multi-dimensional and chemically reacting flows (past Space Shuttle orbiter),” in *Proceedings of 11th International Symposium 1979*, pp. 365–388.
[25] S. J. Plimpton *et al.*, “Direct simulation Monte Carlo on petaflop supercomputers and beyond,” *Physics of Fluids*, 31(1), p. 86101, 2019.
[26] J. M. Burt and I. D. Boyd, “High altitude plume simulations for a solid propellant rocket,” *45th AIAA Aerospace Sciences Meeting and Exhibit*, AIAA 2007-1013, pp. 1–17, 2007.
[27] P. W. Erdman *et al.*, “In-situ measurements of UV and VUV radiation from a rocket plume and reentry bow shock,” *30th Aerospace Sciences Meeting and Exhibit*, AIAA 92-014, pp. 1–14, 1992.